ISSN 0031-918X, The Physics of Metals and Metallography, 2015, Vol. 116, No. 10, pp. 967–978. © Pleiades Publishing, Ltd., 2015.
Original Russian Text © M.P. Kashchenko, V.G. Chashchina, 2015, published in Fizika Metallov i Metallovedenie, 2015, Vol. 116, No. 10, pp. 1019–1030.

THEORY OF METALS

# Dynamic Interpretation of the Orientation Relationships Arising upon the α–ε–γ Martensitic Transformation via the Transformation of $\{112\}_\alpha$ Planes

**M. P. Kashchenko[a, b] and V. G. Chashchina[a, b]**

[a] *Yeltsin Ural Federal University (UrFU), ul. Mira 19, Ekaterinburg, 620002 Russia*
[b] *Ural State Forest Engineering University, Sibirskii trakt 37, Ekaterinburg, 620100 Russia*
*e-mail: mpk46@mail.ru*

Received November 5, 2014; in final form February 25, 2015

**Abstract**—In this work, we have considered different variants of the formation of martensite crystals upon the α–ε transformation caused by the deformation of planes $\{112\}_\alpha$ that leads to the symmetry of atomic arrangement typical of the basal planes $\{0001\}_\varepsilon$ of the ε phase within the dynamic theory of martensitic transformations. It has been shown that there are dislocation nucleation centers that facilitate the start of the wave process responsible for the initiation of this deformation. The relatively rarely observed parallelism of three planes of different phases, namely, $\{112\}_\alpha \| \{0001\}_\varepsilon \| \{112\}_\gamma$, is interpreted as a consequence of the rapidly arising unstable intermediate state, which leads to the formation of coherently matched crystals of the γ and ε phases. The opportunity of the existence of the lattice parameter $a_{\varepsilon_2}$ that exceeds the lattice parameter of the α phase is noted.

*Keywords*: martensitic α–ε transformation, dynamic theory, material orientational relationships

**DOI:** 10.1134/S0031918X15100075

## INTRODUCTION

Within the dynamic theory of martensitic transformations (MTs) based on the new paradigm of MTs (see, e.g., [1–4], good agreement with the experimental data for titanium was obtained using the variant of the α–ε MT in which a central role is played by the plane deformation of the tension–compression of $\{110\}_\alpha$ planes [5, 6]. This deformation is initiated by a pair of waves (responsible for the description of the crystal habits) with an additional shuffling of the deformed planes. This shuffling (inhomogeneous shear of each second plane) does not affect the macroscopic morphological characteristics; therefore, we will not focus further attention on it. In the structure of the controlling wave process (CWP), the normal $\boldsymbol{n}_1$ ($|\boldsymbol{n}_1| = 1$) is connected with certainty that the wave that carries the threshold tensile deformation ($\varepsilon_1 > 0$), and $\boldsymbol{n}_2$ ($|\boldsymbol{n}_2| = 1$) is related to the wave that initiates compressive strain ($\varepsilon_2 < 0$). The CWP starts [1–4] from the appearance of an initial excited state (IES) in the elastic field of the dislocation nucleation center (DNC). The IES region is naturally determined by the extrema of the elastic deformations, the angular and radial localization of which (in the cylindrical coordinate system) depends on the Burgers vectors and configuration of the DNC. It has been shown that the deformation field of the DNC in the region of the localization of the IES can be inherited by the CWP. In this case, the structure of the CWP becomes completely determined. In particular, the direction of the principal deformations $\xi_{1w}$ and $\xi_{2w}$ ($|\xi_{1,2w}| = 1$) of the tensor $\hat{\varepsilon}_w$ of deformations [7] carried by the CWP coincides with the eigenvectors $\xi_1$ and $\xi_2$ ($|\xi_{1,2}| = 1$) of the tensor $\hat{\varepsilon}$ of deformations of the elastic field of the DNC.

In the general case, the wave normals $\boldsymbol{n}_{1,2}$ do not coincide with the symmetry axes, and the waves are quasi-longitudinal. Then, the principal axes $\xi_{1,2w}$ of the tensor of deformation $\hat{\varepsilon}_w$ of the transferred CWP are oriented in the directions that are intermediate with respect to both the wave normals and the polarization vectors of the waves [7].

An important condition for transitioning from the threshold deformations ($\varepsilon_{th}$) to the final deformations ($\varepsilon_f$) is the requirement that their ratio $k$ remains unaltered, i.e.,

$$k_{th} = (\varepsilon_{1th}/|\varepsilon_{2th}|)^{1/2} = k_f = (\varepsilon_{1f}/|\varepsilon_{2f}|)^{1/2}. \quad (1)$$

The fulfillment of the requirement (1) (at the indicated orientations of the deformation axes $\xi_{1,2}$) supplements the condition of the connection between the deformations $\varepsilon_{1f}$ and $|\varepsilon_{2f}|$ imposed by the condition of

the symmetry of the atomic arrangement in the initial and transformed planes as follows:

$$F(\varepsilon_{1f}, \varepsilon_{2f}) = 0. \quad (2)$$

For example, upon the transformation $\{110\}_\alpha \to \{0001\}_\varepsilon$ and at the orientations of the axes of tension and compression along the symmetry axes $\langle 1\bar{1}0\rangle_\alpha$ and $\langle 001\rangle_\alpha$, respectively, condition (2) takes on the following explicit form:

$$(1-|\varepsilon_2|)\sqrt{3} = (1+\varepsilon_1)\sqrt{2}. \quad (3)$$

If the deformation axes $\xi_{1,2}$ deviate from the symmetry axes by an angle $\theta$ (but remain in the symmetry plane), instead of (3), we can obtain [8]

$$\Gamma_\xi(\theta) = \frac{1+\varepsilon_1}{1-|\varepsilon_2|} = \left[(3-2\tan^2(\theta))/(2-3\tan^2(\theta))\right]^{1/2}, \quad (4)$$

$$-\arctan\sqrt{2/3} < \theta < \arctan\sqrt{2/3}. \quad (5)$$

Upon the transformation $\{110\}_\alpha \to \{0001\}_\varepsilon$, it is natural to expect the parallelism of precisely these planes in the interphase orientation relationships (ORs). In the case of the relationships (3) or close to them, as follows from the dynamic theory of MTs, the ORs are close to material ORs (MORs) as shown below [6]:

$$\begin{gathered}\{011\}_\alpha \| \{0001\}_\varepsilon. \\ |\Delta\varphi(æ)| = \left|\langle 1\bar{1}1\rangle_\alpha \wedge \langle 11\bar{2}0\rangle_\varepsilon\right| \le 0.5^\circ.\end{gathered} \quad (6)$$

In (6), $æ = v_2/v_1$ is the ratio of the moduli of the wave velocities, which is expressed through the elastic moduli of the material of the initial phase. The transition from the MORs-1 (6) to the Burgers ORs is only possible at a specific value $æ = \sqrt{2}$, when the value of $\Delta\varphi(æ) = 0$. Usually, the most close-packed directions are selected as the corresponding directions in ORs. However, as was shown in [8], at large $\theta$ a smaller misorientation of noncorresponding directions is possible, e.g., in the case of the MORs-2

$$\begin{gathered}\{1\bar{1}0\}_\alpha \| \{0001\}_\varepsilon, \\ |\Delta\varphi(æ)| = \left|\langle 110\rangle_\alpha \wedge \langle 1\bar{2}10\rangle_\varepsilon\right| \approx 1^\circ,\end{gathered} \quad (7)$$

which are an analog of the Headley–Brooks ORs [9–11] at $|\Delta\varphi(æ)| = 0$ and pass into these ORs at the $\varepsilon$–$\gamma$ MT (if the mechanism of the $\varepsilon$–$\gamma$ MT does not change the morphological characteristics [12]). In addition, it should be noted that MORs-2 have been obtained in the case of $\Gamma_\xi(\theta) = 2$, $\theta \approx 35.3^\circ$ as follows:

$$\xi_1 = \sqrt{1/3}[111]_\alpha, \ \ \xi_2 = \sqrt{1/6}[11\bar{2}]_\alpha, \quad (8)$$

i.e., the unit vector $\xi_1$ is collinear to the threefold symmetry axis $[111]_\alpha$. To obtain estimates of the deformation levels, it is convenient to use the approximation of an elastically isotropic medium, for which, as was discussed in [8],

$$æ = k_{th} = (\varepsilon_{1th}/|\varepsilon_{2th}|)^{1/2} = k_f = (\varepsilon_{1f}/|\varepsilon_{2f}|)^{1/2} = 1. \quad (9)$$

Then, it follows from (4) and (9) that

$$\varepsilon_{1f} = |\varepsilon_{2f}| = (\Gamma_\xi(\theta) - 1)/(\Gamma_\xi(\theta) + 1). \quad (10)$$

From (10) at $\Gamma_\xi(\theta) = 2$, we obtain $\varepsilon_1 = |\varepsilon_2| = 1/3$.

Since the MORs-2 are indeed observed, although relatively rarely, there are grounds to assume that such a high level of deformations is capable to cause transformation of even less close-packed atomic planes.

The main purpose of this work is to study different variants of the transformation of $\{112\}_\alpha$ planes, in particular, for obtaining MORs supplementary to MORs-1 (6) and MORs-2 (7) that were established in [9, 10]. The existence of several different types of ORs for the reverse (upon slow heating) MTs in the Fe–(30–33)Ni alloys, where the $\varepsilon$ phase was revealed [9, 10] as an intermediate phase upon the $\alpha$–$\gamma$ (bcc–fcc) MT is dictated by the different variants of the start of the CWP in the fields of the defects of lenticular crystals of the $\alpha$ phase. In particular, in [10], crystals of the $\varepsilon$ phase were revealed that were formed upon heating in the partly twinned region that adjoins the single-crystal midrib of the crystals of the initial $\alpha$ phase. Since the twinning plane is parallel to $\{112\}_\alpha$, then, under the conditions compatible with the existence of two variants of twinning of thin martensite plates, the formation of the $\varepsilon$ phase can occur if the CWP initiates a tension–compression deformation of $\{112\}_\alpha$ planes. The parallelism of planes $\{112\}_\alpha \| \{0001\}_\varepsilon$ discovered in [10] indicates the need to analyze the possibility of the $\{112\}_\alpha \to \{0001\}_\varepsilon$ transformation.

In reality, the situation observed in [10] is even richer, since there is an additional important feature (realized for a small fraction of crystals), namely, the possibility of a parallelism of the planes of three phases, i.e., $\{112\}_\alpha \| \{0001\}_\varepsilon \| \{112\}_\gamma$.

### *Conditions for the* $\{112\}_\alpha \to \{0001\}_\varepsilon$ *Transformation*

In the $(112)_\alpha$ plane, a pair of orthogonal directions $[11\bar{1}]_\alpha$ and $[1\bar{1}0]_\alpha$ specifies a network in which the spacings between the atoms located in neighboring sites are $a_\alpha\sqrt{3}/2$ and $a_\alpha\sqrt{2}$, where $a_\alpha$ is the lattice parameter of the $\alpha$ phase. Let us consider a hexagonal cell *ABCDEF* that consists of six right-angled triangles in the $(112)_\alpha$ plane, as is shown in Fig. 1.

The sides of the cell are equal pairwise (in the $a_\alpha$ units) as follows: $AB = DE = \sqrt{3}/2$, $BC = EF = \sqrt{2}$, $CD = FA = \sqrt{11}/2$. It is obvious that there is one additional mirror-symmetrical (with the reflection in the $(1\bar{1}0)_\alpha$ plane) variant of the choice of a hexagonal cell. It can be seen from Fig. 1 that the segment *AC* is not orthogonal to *BE*. The elementary trigonometry yields for the angle $\psi$ between *AC* and the normal to *BE* a

value $\tan\psi = 5/11$, i.e., $\psi \approx 24.44°$. It is possible to transform cell *ABCDEF* into a cell of the ε phase that consists of six equilateral triangles through an intermediate state (IS), in which the hexagonal cell *A'B'C'D'E'F'* consists of six isosceles right-angled triangles. It can easily be understood that the $IS_{\alpha-\varepsilon}$ is characterized by a network of sites, in which *A'C'* and *B'E'* are orthogonal as the diagonals of a rhombus. In turn, the formation of the $IS_{\alpha-\varepsilon}$ is possible by different methods.

For example, it can be reached via pure shear $\tan\psi = 5/11$ (without a change in the lengths of the sides *CD* and *FA* and in the distance between them) in the direction

$$S \parallel [\sqrt{2}+1,\ 1-\sqrt{2},\ \bar{1}]_\alpha. \tag{11}$$

Note that an analogous variant of shear for the mirror-symmetrical cell in the direction

$$S \parallel [1-\sqrt{2},\ \sqrt{2}+1,\ \bar{1}]_\alpha \tag{12}$$

is alternative to the initial variant of the cell, giving an $IS1_{\alpha-\varepsilon}$ (without a change in the lengths of the segments *AC* and *FD* and in the distances between them) with the orthogonal orientations *A'C'* and *B'E'* at the same magnitude of the shear $\tan\psi$.

After the shear (11), the cell of the $IS1_{\alpha-\varepsilon}$ can be converted into a cell that consists of six equilateral triangles via the deformation of tension–compression along the orthogonal directions collinear to *A'C'* and *B'E'* as follows:

$$\begin{gathered}\xi_{1\alpha} \parallel [2\sqrt{2}-3,\ 2\sqrt{2}+3,\ -2\sqrt{2}]_\alpha,\\ \xi_{2\alpha} \parallel [\sqrt{2}+1,\ 1-\sqrt{2},\ \bar{1}]_\alpha,\end{gathered} \tag{13}$$

or in the normalized form

$$\begin{aligned}\xi_{1\alpha} &= [\overline{0.026474}\ \ 0.899346\ \ \overline{0.436436}]_\alpha,\\ \xi_{2\alpha} &= [0.912487\ \ \overline{0.156558}\ \ \overline{0.377964}]_\alpha.\end{aligned} \tag{14}$$

Note that, to obtain the second variant of the choice of the hexagonal cell in the description of the directions of the vectors of tension and compression, it is sufficient in (14) to interchange the positions of the first and second projections.

Upon the orientations of the deformation axes given by (14), the deformations of tension ($\varepsilon_1$) and compression ($\varepsilon_2$) satisfy the following relationship:

$$\Gamma_1 = (1+\varepsilon_1)/(1-|\varepsilon_2|) = 11/(4\sqrt{2}). \tag{15}$$

Let us now assume that the shear $\tan\psi = 5/11$ is accompanied by an additional tension along $\xi_{1\alpha}$, which ensures the equality of the segments $A'C' = AC$. This corresponds to the transition to an $IS2_{\alpha-\varepsilon}$ with a square network of sites. Then, the deformation of the tension–compression along the directions (13) is characterized by the relationship

$$\Gamma_2 = (1+\varepsilon_1)/(1-|\varepsilon_2|) = \sqrt{3}. \tag{16}$$

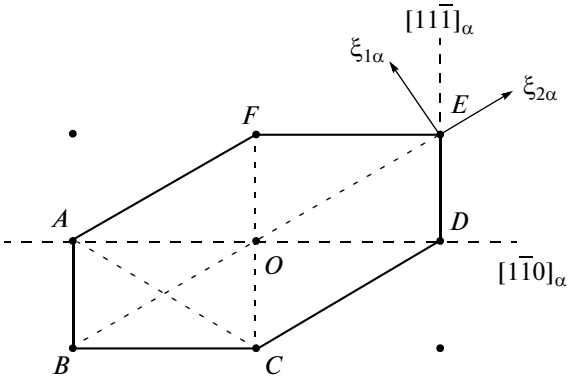


**Fig. 1.** Choice of a hexagonal cell in the plane $(112)_\alpha$.

We should bear in mind that, in (14) and (15), just as in (3), the ratio of the deformations $\varepsilon_1/|\varepsilon_2|$, can in principle have any value from the interval $(0, \infty)$. For example, in the case of the uniaxial compression at $\varepsilon_1 = 0$, from (15) we find the maximum permissible value $|\varepsilon_2|_m$ upon the transition to the ideal ε phase for the transformation $\{112\}_\alpha \to \{0001\}_\varepsilon$ as follows:

$$|\varepsilon_2|_m = 1 - (4\sqrt{2}/11) \approx 0.48574 \tag{17}$$

(similarly, it follows from (16) that $|\varepsilon_2|_m = 1 - (1/\sqrt{3}) \approx 0.42265$).

In the general case, the concrete ratio of deformations is assigned by the threshold regime.

The estimation in the model of an elastically isotropic medium for the $IS_{\alpha-\varepsilon} \to \varepsilon$-phase transition with allowance for (10) gives for the case (15)

$$\varepsilon_{1f} = |\varepsilon_{2f}| = (11-4\sqrt{2})/(11+4\sqrt{2}) \approx 0.32, \tag{18}$$

and, for the case (16),

$$\varepsilon_{1f} = |\varepsilon_{2f}| \approx (1-\Gamma_2)/(1+\Gamma_2) \approx 0.27. \tag{19}$$

In (18) and (19), the final deformations are counted-off from the $IS_{\alpha-\varepsilon}$ state in the assumption that the orientation $\xi_{2\alpha} \parallel S$ during the shear remains unaltered. It is quite probable that the shear that gives the $IS_{\alpha-\varepsilon}$ very is realized most rapidly, i.e., in the wave regime. A change in the configuration of the network of sites indicates that the mechanism of shear can be caused by the propagation of the tension–compression deformation along the symmetry axes $[11\bar{1}]_\alpha$ and $[1\bar{1}0]_\alpha$.

Indeed, when the MT occurs under constrained conditions (in the transformation channel surrounded by a metastable initial phase), the lattice rotates as a whole, which is accompanied by a macroshear with the basic component $S_\tau$ in the habit plane. According to [7], $S_\tau$ is collinear to the vector sum $\mathbf{v} = \mathbf{v}_1 + \mathbf{v}_2$ of the orthogonal velocities $\mathbf{v}_{1,2}$ of the pair of controlling waves. The orientation of $S_\tau$ can coincide with $S$ (11). Indeed, in the approximation of the elastically isotro-

pic medium, the velocity $\boldsymbol{v}$ is collinear to the bisectrix of the angle between the vectors $\mathbf{v}_1$ and $\mathbf{v}_2$, i.e., makes angles equal to ±45° with them. The angle between $S \parallel \xi_{2\alpha}$ and $[11\bar{1}]_\alpha$ is equal to ≈49.1° (correspondingly, the angle between $S$ and $[1\bar{1}0]_\alpha$ is equal to ≈40.9°). It is clear that with allowance for the anisotropy of elastic properties (velocity $\boldsymbol{v}_\Lambda$ along $11\bar{1}]_\alpha$ is greater than the velocity $\boldsymbol{v}_\Sigma$ along $[1\bar{1}0]_\alpha$), in principle, there is a ratio of the moduli of the velocities $v_\Lambda/v_\Sigma$ (let us designate it æ*) at which the relation (11) is fulfilled precisely. The relation (11) can also be fulfilled upon the deviation of the velocities $\mathbf{v}_1$ and $\mathbf{v}_2$ from the symmetry axes. It is clear that in the approximation of an elastically isotropic medium the deviation is about 4°. In the real anisotropic medium, the deviation can be connected with the orientation of the Burgers vector of the DNC, the elastic field of which specifies the region favorable for the appearance of an IES.

It is expedient to recall that the planes $\{110\}_\alpha$, $\{112\}_\alpha$, and $\{123\}_\alpha$ in the α phase have close densities of atomic packing. Therefore, in the regions where the channel of the plane deformation of the most close-packed planes of the α phase, i.e., $\{110\}_\alpha$, is not activated, there is possible a rapid transformation of the plane $\{112\}_\alpha$, although at greater values of deformations compared with the case of the deformation of planes $\{110\}_\alpha$. One should bear in mind that, with the rejection of the requirement of the ideality of the lattice of the ε phase, the value of the shear can be less than 5/11. In fact, the sequence of the two above-described deformation stages may also be the opposite. In this case, much depends on which of the dynamic variants of the appearance of an IES is the first to be achieved.

### *Conditions for the Deformation-Induced* $\{112\}_\alpha \to \{112\}_\gamma$ *Transition*

The parallelism of the planes $\{112\}_\alpha \parallel \{0001\}_\varepsilon \parallel \{112\}_\gamma$ established in [10] indicates the opportunity of the direct transformation $\{112\}_\alpha \to \{112\}_\gamma$. The network of atomic sites in the plane $(112)_\gamma$ is characterized by analogous symmetry axes; however, closely packed atomic rows are associated with the $[1\bar{1}0]_\gamma$ axis with spacings $a_\gamma/\sqrt{2}$ between the nearest sites ($a_\gamma$ is the lattice parameter of the γ phase). Along the $[11\bar{1}]_\gamma$ axis, spacing between the sites is equal to $a_\gamma\sqrt{3}$. Assume that the transition from one atomic network to another occurs by the shortest path according to the tension–compression scheme along the axes $[1\bar{1}0]_\alpha$ and $[11\bar{1}]_\alpha$, respectively. In this case, we obtain the following connection between the deformations:

$$\Gamma_3 = (1 + \varepsilon_1)/(1 - |\varepsilon_2|) = 3/2. \qquad (20)$$

In the model of the elastically isotropic medium, we have

$$\varepsilon_{1f} = |\varepsilon_{2f}| = (\Gamma_3 - 1)/(1 + \Gamma_3) = 0.2. \qquad (21)$$

Then, the lattice parameter

$$a'_\gamma = \sqrt{\frac{3}{2}}(1 - |\varepsilon_2|_{\alpha-\gamma})a_\alpha \approx 0.979796a_\alpha \sim a_\alpha \qquad (22)$$

turns out to be anomalously small compared with the typical values of $a_\gamma$, which exceed $a_\alpha$ by ~0.25$a_\alpha$.

We should emphasize that the expected relation is $a_\gamma \approx 1.26a_\alpha$, which follows from the requirement of the equality of the volumes per atom:

$$a_\gamma^3/4 = a_\alpha^3/2 = (4\pi/3)(r_0)^3, \qquad (23)$$

where $r_0$ is the effective atomic radius. According to [13], the value $r_0$ is bounded from below by a value $r_{0\min}$, which assigns the minimum atomic volume in the absence of significant external pressures at a constant electron configuration of the atom (for example, for the iron atom with the assumed configuration $3d^74s^1$, we have $(r_{0\min})_{Fe} \approx 1.41$ Å). It follows from (23) that

$$a_\gamma = (2)^{1/3}a_\alpha \approx 1.26a_\alpha, \qquad (24)$$

and the minimum values of the parameters of the cubic lattices permitted for Fe are

$$\begin{aligned}(a_{\alpha\min})_{Fe} &= (8\pi/3)^{1/3}(r_{0\min})_{Fe} \approx 2.863685 \text{ Å},\\ (a_{\gamma\min})_{Fe} &= (2)^{1/3}(a_{\alpha\min})_{Fe} \approx 3.608018 \text{ Å}.\end{aligned} \qquad (25)$$

Since the effective atomic radius of Ni is $(r_{0\min})_{Ni} \approx$ 1.38 Å, i.e., less than that of Fe, the minimum average lattice parameters of concentrated Fe–Ni alloys will be less than the values given in (25). It is pertinent to recall that precisely such an approach makes it possible to connect the observed [14] value of the $M_s$ temperature upon the rapid cooling with the lower boundary of the start of the MT, at which $a_\gamma$ reaches the value $(a_\gamma)_{\min}$ [15]. It is clear that under the assumption about the retention of the electron configuration of atoms upon the deformation of planes $(112)_\alpha$, the formally obtained anomalously low estimations (22) for $a'_\gamma$ cannot be realized. Even in the case of $|\varepsilon_2|_{\alpha-\gamma} = 0$, $a'_\gamma = (a'_\gamma)_{\max} = \sqrt{\frac{3}{2}}$, and $a_\alpha \approx 1.224745a_\alpha$. Note also that, in the case of the formation (in the course of slow heating that does not suppress the diffusion of the components of the Fe–32Ni alloy) of local regions with the ordering of the α phase according to the $B2$ type, the value of the parameter $a_\alpha$ can decrease only to $a'_\alpha \approx 2.833221$ Å, so that $(a'_\gamma)_{\max}$ will become equal to $\approx 1.237914a'_\alpha$. This means that, with the requirement of the transformation of the $[11\bar{1}]_\alpha$ axis into the $[1\bar{1}0]_\gamma$ axis, not the

compressive strain $\varepsilon_2$, but rather tensile deformation $\varepsilon'_2 > 0$ is required, which satisfies the condition

$$a_\gamma = (2)^{1/3} a_\alpha = \sqrt{\frac{3}{2}}(1 + \varepsilon'_2|_{\alpha-\gamma}) a_\alpha. \quad (26)$$

From (26), we find that $\varepsilon'_2 \approx 0.028721$. In the approximation of the isotropic medium, $\varepsilon'_2 = \varepsilon'_1$. This means that the final (≈0.03) tensile deformations in the orthogonal $[11\bar{1}]_\alpha$ and $[1\bar{1}0]_\alpha$ directions can be initiated by the CWP and rapidly develop, forming a band of an intermediate state $IS1_{\alpha-\gamma}$. For the transition from the $IS1_{\alpha-\gamma}$ to the atomic configuration characteristic of the plane $(112)_\gamma$, there is required a tension $(\varepsilon_1 - \varepsilon'_1)_1$ in the direction $[1\bar{1}0]_\alpha$, which can easily be estimated by substituting $(1 + |\varepsilon_2|)$ in (20) for $(1 - \varepsilon'_2)$:

$$\begin{aligned} \varepsilon_1 &= (3/2)(1 + \varepsilon'_2) - 1, \\ (\varepsilon - \varepsilon'_1)_1 &= (1/2)(1 + \varepsilon'_2) \approx 0.514360. \end{aligned} \quad (27)$$

Thus, the unstable $IS1_{\alpha-\gamma}$ state can initiate compressive deformation in the $[1\bar{1}0]_\alpha$ direction in the regions of the $(112)_\alpha$ plane that adjoin the $IS1_{\alpha-\gamma}$ band. As was discussed above, the $IS_{\alpha-\varepsilon} \to \varepsilon$-phase transition for the planes $(112)_\alpha$ can occur via pure compression along the direction $\xi_{2\alpha}$ at deformations of ≈0.48574 (17) (or ≈0.42265). Therefore, the scenario of the appearance of the ε phase in the bands of the $IS_{\alpha-\varepsilon}$ in the course of the expansion of the $IS1_{\alpha-\gamma}$ bands seems to be quite real. It is obvious that the smaller the angle between $\xi'_{2\alpha}$ (in the process of shear, there occurs a change in the orientation: $\xi_{2\alpha} \to \xi'_{2\alpha}$) and the direction of compression, the greater the efficiency of the compression process.

For comparison, let us now examine the variant of the deformation-induced transition to $IS2_{\alpha-\gamma}$ that preserves the correspondence of the symmetry axes

$$[1\bar{1}0]_\alpha \| [1\bar{1}0]_\gamma, \ [11\bar{1}]_\alpha \| [11\bar{1}]_\gamma$$

due to the expansion along $[11\bar{1}]_\alpha$ and compression along $[1\bar{1}0]_\alpha$.

In this case, we obtain the relationships

$$\frac{\sqrt{3}}{2}(1 + \varepsilon_1) a_\alpha = \sqrt{3} a_\gamma; \quad (28)$$

$$\sqrt{2}(1 - |\varepsilon_2|) a_\alpha = \frac{\sqrt{2}}{2} a_\gamma; \quad (29)$$

$$\Gamma_4 = (1 + \varepsilon_1)/(1 - |\varepsilon_2|) = 4. \quad (30)$$

With the fulfillment of condition (24), we find from (29) that $|\varepsilon_2| = 1 - 2^{-2/3} \approx 0.370039$. In the approximation of the isotropic medium, there corresponds a relation $\varepsilon'_1 = |\varepsilon_2|$ and $IS2_{\alpha-\gamma}$ to this value of $|\varepsilon_2|$. It is natural to consider this value of $|\varepsilon_2|$ to be a threshold value. According to (30), the $IS2_{\alpha-\gamma} \to \gamma$ transition will be accompanied by the additional expansion $(\varepsilon_1 - \varepsilon'_1)_2$ as follows:

$$(\varepsilon_1 - \varepsilon'_1)_2 = 4(1 - |\varepsilon_2|) - 1 - \varepsilon'_1 = 3\text{–}5|\varepsilon_2| \approx 1.149803. \quad (31)$$

Taking into account these estimates, we can assume that the magnitudes of the threshold deformations for the $IS1_{\alpha-\gamma}$ are less by an order of magnitude than those for the $IS2_{\alpha-\gamma}$. From the point of view of this factor, the $IS1_{\alpha-\gamma}$ state is more advantageous. However, from the point of view of the magnitude of the angle between $\xi'_{2\alpha}$ and the direction of compression, the $IS2_{\alpha-\gamma}$ variant may prove to be more efficient, despite that the initial orientation of $\xi_{2\alpha}$ makes an angle with the $[11\bar{1}]_\alpha$ axis that is 8.2° greater than that with $[1\bar{1}0]_\alpha$. Indeed, in view of the equal tensile deformations in the orthogonal directions, the transition to $IS1_{\alpha-\gamma}$ is not accompanied by the rotation of the lattice inside the $IS1_{\alpha-\gamma}$ band and, consequently, does not change the orientation of $[1\bar{1}0]_\alpha$. On the contrary, the transition to $IS2_{\alpha-\gamma}$ is accompanied by significant shear and by the rotation of the lattice inside the $IS2_{\alpha-\gamma}$ band and changes the orientation $[11\bar{1}]_\alpha$ into $[11\bar{1}]'_\alpha$. As a result, the angle between $[11\bar{1}]'_\alpha$ and $\xi'_{2\alpha}$ will be equal to ≈4.35°, whereas the angle between $[1\bar{1}0]_\alpha$ and $\xi'_{2\alpha}$ will be ≈16.46°. Of course, these estimations were carried out under the assumption that the CWP initiates deformation strictly along the symmetry axes. However, depending on the IES, the directions of deformations can deviate noticeably from the symmetry axes.

Note that the formation of ISs in the form of pairs of conjugate bands (plates) of $IS_{\alpha-\gamma}$ and $IS_{\alpha-\varepsilon}$ can occur in a synchronized regime upon the formation of a pair of IESs, as is schematically shown in Fig. 2.

It is clear from the configuration of displacements shown in Fig. 2 that it is a variant that corresponds to the appearance of a tandem of bands of the $IS2_{\alpha-\gamma}$ and $IS2_{\alpha-\varepsilon}$ states. Note that the scheme bears a simplified nature (is given only for the illustration); in the more realistic variant, the appearing bands will be separated by an interlayer of an untransformed (but strongly distorted) α phase.

### *Estimations for Morphologic Characteristics in the Approximation of Elastically Isotropic Medium*

For certainty, let us assume that the first stage of an MT is connected with the formation of a distorted ε phase obtained via the tension–compression along the axes given by (14).

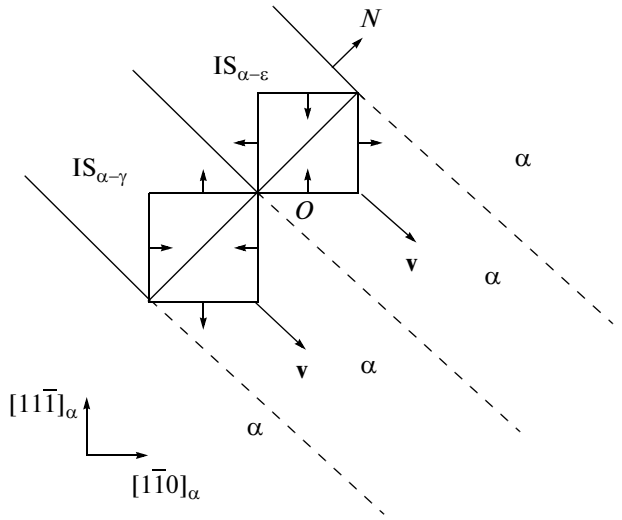


**Fig. 2.** Scheme illustrating the appearance of an IS upon the synchronous starting of the formation of IS1$_{\alpha-\gamma}$ and IS$_{\alpha-\varepsilon}$ bands.

Then, based on [6–8], for the α–ε MT, we can expect the formation of MORs-3 as follows:

$$\{112\}_\alpha \parallel \{0001\}_\varepsilon,$$
$$\langle 11\bar{1}\rangle_\alpha \wedge \langle 01\bar{1}2\rangle_\varepsilon = \Delta\varphi_3(æ) = \varphi_{03} - \varphi(æ), \quad (32)$$

$$\varphi_{03} = \arctan[\sqrt{3}/(2\sqrt{2})] - \arctan[\sqrt{3}/(2\sqrt{2}\Gamma_1)],$$
$$\varphi(æ) = \arctan(æ) - \arctan(æ/\Gamma_1). \quad (33)$$

When writing the expression for $\varphi_{03}$, it was taken into account that, according to the scheme given in [7], the sides of the rectangular cell prior to deformation are collinear to the directions (14), and one of the diagonals is collinear to $\langle 11\bar{1}\rangle_\alpha$. It follows from (15), (32), and (33) at æ = 1 that $\varphi_{03}$ is ≈14°, φ(æ) is ≈17.8° and, consequently, $\Delta\varphi_3(æ) \approx -3.8°$. Thus, in the case of the α–ε MT for the crystals of the γ phase with MORs-3 (32), there are expected misorientations $\Delta\varphi_3(æ)$ between the corresponding directions $\langle 11\bar{1}\rangle_\alpha$ and $\langle 01\bar{1}\rangle_\gamma$ that are significant compared to $\Delta\varphi_1$ in the MORs-1 (6).

The other morphological characteristics from the standard list also differ noticeably., According to [1–4], the normals to the habit planes at æ = 1 are reduced to the sums and differences in the unit wave normals $\boldsymbol{n}_{1,2}$. This means that, at $\boldsymbol{n}_1 = \xi_{1\alpha}$ and $\boldsymbol{n}_2 = \xi_{2\alpha}$, where $\xi_{1,2\alpha}$ are taken from (14), the expected orientations of the normals to the habits are

$$N_{1,2} \parallel \boldsymbol{n}_2 \pm æ n_1 \parallel \boldsymbol{n}_2 \pm \boldsymbol{n}_1. \quad (34)$$

From (34) and (14), we obtain the following expressions for the normalized vectors:

$$N_1/|N_1| = [0.626506\ \ 0.525230\ \ \overline{0.575868}]_\alpha, \quad (35)$$

$$N_2/|N_2| = [0.663946\ \ \overline{0.746637}\ \ 0.0413459]_\alpha, \quad (36)$$

or, in the approximation of small integer indices, $N_1 \parallel [14\ 12\ \overline{13}]_\alpha \sim [11\bar{1}]_\alpha$ and $N_2 \parallel [16\ \overline{18}\ 1]_\alpha \sim [1\bar{1}0]_\alpha$; moreover, the plane $\{112\}_\alpha$ that enters into the MORs-3 is orthogonal to the habit planes. For the untwinned crystals, the macroshear in the dynamic theory [7] is written as

$$\tan\varphi' = æ|\varepsilon_2| = \sqrt{\varepsilon_1|\varepsilon_2|} = \varepsilon_1/æ. \quad (37)$$

Then, from (37), at $\varepsilon_1 = |\varepsilon_2| = 0.32$, we obtain $\tan\varphi' = 0.32$.

If the first stage is connected with the transition to IS1$_{\alpha-\gamma}$, then, without taking into account the deviations of $\boldsymbol{n}_{1,2}$ from the symmetry axes, we have, according to (34), the following estimates for the normals to the habit planes:

$$N_1/|N_1| = [0.908248\ \ \overline{0.0917517}\ \ \overline{0.408248}]_\alpha, \quad (38)$$

$$N_2/|N_2| = [\overline{0.0917517}\ \ 0.908248,\ \ \overline{0.408248}]_\alpha, \quad (39)$$

or, in the approximation of integer indices, $N_1 \parallel [20\ \bar{2}\ \bar{9}]_\alpha \sim [2\ 0\bar{1}]_\alpha$ and $N_2 \parallel [\bar{2}\ 20\ \bar{9}]_\alpha \sim [0\ 2\ \bar{1}]_\alpha$. The habits (38) and (39) differ significantly from (35) and (36); therefore, reliable experimental information about the habits of the crystals of the ε phase with the MORs-3 will make it possible in each concrete case to establish the sequence of deformation stages.

Note that MORs-3 (32) require the formation of the ε phase due to tension–compression along the axes given in (14). Furthermore, the calculation of the elastic field of the DNC makes it possible to select one variant from the pairs of potentially possible habits, which satisfies the requirement of the maximum shear [4]. Naturally, upon comparison with the experiment, the allowance for the elastic anisotropy, just as for possible deviations of $\boldsymbol{n}_{1,2}$ from the symmetry axes, is important. Therefore, the above estimates are only approximate guides for conducting further calculations and analyzing morphological characteristics.

Since the interplanar spacing is proportional to the lattice parameter, the α–γ MT with the $(112)_\alpha \rightarrow (112)_\gamma$ transformation should be accompanied by the expansion in the $[112]_\alpha$ direction. This expansion is in the equal measure necessary both upon the selection of the mirror-symmetrical variant of the hexagonal cell and upon the tensile deformation along the orthogonal $[1\bar{1}0]_\alpha$ (or $[11\bar{1}]_\alpha$) direction. The most optimum variant is that of the formation of layered structures (LSs) (similar to transformation twins [7, 16–18]) that arise due to the concerted action of relatively long-

wavelength displacements (*l* waves) with the wave normal along $[112]_\alpha$ and $[1\bar{1}0]_\alpha$ (or $[112]_\alpha$ and $[11\bar{1}]_\alpha$) with relatively short-wavelength displacements (*s* waves) that initiate the $\alpha \to IS_{\alpha-\gamma}$ transition. Moreover, the role of the main component of the twin structure is played by the plate of the γ phase, and the role of the additional component, by the ε phase. Since the MT occurs at elevated temperatures, the realization of these LSs is prevented by the significant damping of the *s* waves. Nevertheless, this coordination is quite possible; therefore, the detection of the corresponding nanocrystalline fragments of the ε phase is of great interest. If the phase of the *l* wave, which propagates along the symmetry axis, corresponds to compression, then the role of the main component of the LS will be played by the ε phase, and the role of the additional component is played by the γ phase. Recall that the habit of plates with a layered structure is determined by the *l* waves. Consequently, based on (34), at æ = 1, $\boldsymbol{n}_1 \parallel [112]_\alpha$ and $\boldsymbol{n}_2 \parallel [1\bar{1}0]_\alpha$, we have a pair of habits with the following normals:

$$N_1/|N_1| = [0.788675,\ \overline{0.211325}\ \ 0.577350]_\alpha; \quad (40)$$

$$N_2/|N_2| = [0.211325,\ \overline{0.788675},\ \overline{0.577350}]_\alpha, \quad (41)$$

or $N_1/|N_1| \sim [4\bar{1}3]_\alpha$ and $N_2/|N_2| \sim [1\bar{4}\bar{3}]_\alpha$; whereas at æ = 1 and $\boldsymbol{n}_1 \parallel [112]_\alpha$ and $\boldsymbol{n}_2 \parallel [11\bar{1}]_\alpha$ we also have

$$N_1/|N_1| = [0.696923,\ 0.696923\ \ 0.169102]_\alpha, \quad (42)$$

$$N_2/|N_2| = [0.119573,\ 0.119573,\ \overline{0.985599}]_\alpha, \quad (43)$$

or $N_1/|N_1| \sim [441]_\alpha$ and $N_2/|N_2\| \sim [11\bar{8}]_\alpha$.

If an LS is realized, then the habits (38) or (39) become the orientations of internal boundaries in the crystals with habits (40)–(43).

## ALLOWANCE FOR THE ELASTIC ANISOTROPY

Since the elastic moduli for the α phase of the Fe–32Ni alloy are not known exactly for the temperature range of the reverse MT, we will illustrate the changes in the calculations on a concrete example using the elastic moduli of α-Fe at room temperature as follows (J/kg):

$$C_{11} \approx 23.01,\ C_L \approx 29.895,\ C_{44} \approx 11.66$$
$$(C' = 4.775,\ C_{12} \approx 13.46). \quad (44)$$

As an example, we examine the change in the orientation of the habits (38) and (39) at $\boldsymbol{n}_1 \parallel [11\bar{1}]_\alpha$, $\boldsymbol{n}_2 \parallel [1\bar{1}0]_\alpha$, and

$$æ = v_2/v_1 = [(C_{11} + 2C_{12} + 4C_{44})/3C_L]^{-1/2}. \quad (45)$$

From (45) and (44), we obtain æ = 0.963689. Then, from (34), we obtain

$$N_1/|N_1| = [0.909789\ \ \overline{0.108528}\ \ \overline{0.400631}]_\alpha, \quad (46)$$

$$N_2/|N_2| = [0.108528\ \ \overline{0.909789}\ \ 0.400631]_\alpha. \quad (47)$$

Since the magnitude of æ deviates from 1 only slightly, the deviation of the orientations (46), (47) from (38), (39) is ≈1.06°, i.e., is insignificant.

More substantial changes can be connected with the deviations of the wave normals from the symmetry axes caused by the appearance of IESs in the elastic fields of the DNCs. However, this relates to the case of the independent formation of separate crystals with such habits. However, if these boundaries relate to the internal boundaries of the LSs, then their formation is governed by the *s* waves, which appear via a fluctuation mechanism. Therefore, the phasings of the deformations in the *s* waves by no means necessarily will be strictly coordinated with the phasings of the *l* waves. However, the directions of the propagation of *s* waves can correspond to the symmetry axes, since at other orientations, the level of deformations required for the initiation of MTs must be higher. Therefore, in the case of LSs, we may expect the appearance of precisely above-indicated or close to (38), (39) orientations of internal boundaries.

### *Results of Calculating the Elastic Field of Possible DNCs*

It is useful to examine which of the DNCs correspond to the above schemes of the transformation of $\{112\}_\alpha$ planes and in what measure they correspond to them. The main segment of the dislocation loop of the DNC is chosen with the orientation of $\Lambda_1$ along the normal to the transformed plane $\Lambda_1 \parallel \langle 112\rangle_\alpha$. As the Burgers vectors $\boldsymbol{b}$, it is natural to primarily examine the edge (with respect to $\Lambda_1$) orientations that coincide with the directions of the symmetry axes as follows: $\boldsymbol{b}_1 \parallel \langle 110\rangle_\alpha$, $\boldsymbol{b}_2 \parallel \langle 11\bar{1}\rangle_\alpha$. If we consider dislocation loops, rather than separate segments of dislocation lines $\Lambda_1$ as the DNCs, the minimum distortions of the fields of the segments with the lines $\Lambda_1 \parallel [112]_\alpha$ should be expected for the rectilinear loops with purely screw orientations of $\boldsymbol{b}$ relative to the second segment of the loop $\Lambda_2$, i.e., at $\Lambda_2 \parallel \boldsymbol{b}$. For certainty, let us assume that $\Lambda_1 \parallel [112]_\alpha$ and that $\boldsymbol{b}_1 \parallel [1\bar{1}0]_\alpha$ and $\boldsymbol{b}_2 \parallel [11\bar{1}]_\alpha$. In the calculations of the elastic fields of the DNCs, the elastic moduli (44) will be used, as before.

The spatial arrangement of the cylindrical frame of reference relative to the rectangular dislocation loop with the orientations of the sides specified by the unit vectors $\tau_1$ and $\tau_2$ is given in Fig. 3.

It can be seen from Fig. 3 that the origin is placed in the center of the segment $\Lambda_1$, and the angle θ is

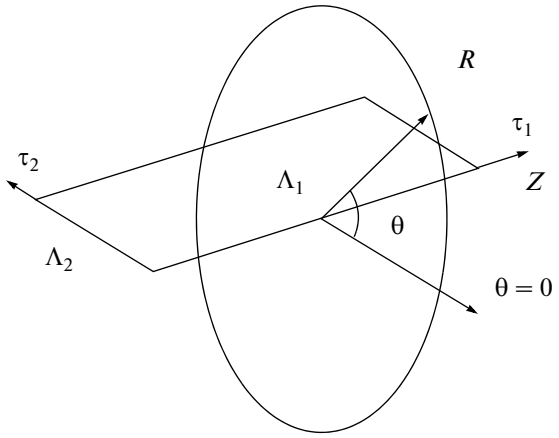


**Fig. 3.** Cylindrical coordinate system used in the calculations of the elastic fields of dislocation loops.

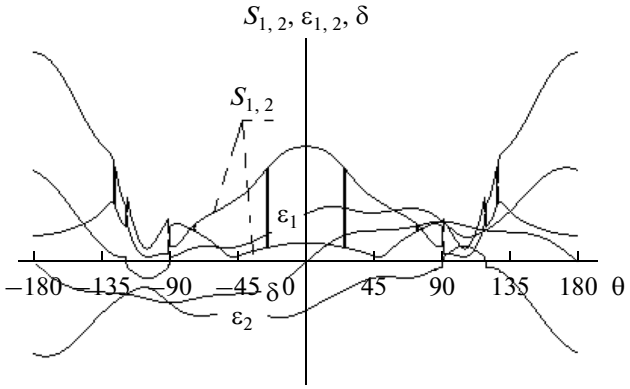


**Fig. 4.** Angular dependences of the magnitudes of the shears $S_{1,2}$, eigenvalues $\varepsilon_{1,2}$ of the tensor of deformations, and change in the relative volume $\delta$ of the elastic field of the DNC at $\boldsymbol{b}_1 \parallel [1\bar{1}0]_\alpha$ for $R = 1200$.

counted off from the plane of the loop. The positive values of θ correspond to the counterclockwise rotation (upon the observation from the end of the vector $\tau_1$). The distance to the observation point $R$ is assigned in the units of the lattice parameter $a$.

Since the plane $(112)_\alpha$ is not a symmetry plane of the cubic lattice, for the case we are interested in (for the axes of compression and tension to be in the plane $(112)_\alpha$), we should find a local region of the elastic field of the DNC in which the third axis $\xi_3$ of the tensor of deformation of the elastic field of the DNC is collinear to $\Lambda_1$.

The above-said is illustrated by the results of calculations for a loop with the lengths of the sides (in units of $a$) $L_1 = 7000$ and $L_2 = 5000$ at $\boldsymbol{b}_1 \parallel [1\bar{1}0]_\alpha$ given in Fig. 4.

Figure 4 displays the angular dependences of the shear $S$, eigenvalues $\varepsilon_{1,2}$ of the tensor of deformations, and relative change $\delta$ in the volume of the elastic field of the DNC at $R = 1200$. The vertical lines in Fig. 4 separate the regions, in which the sign in the inequality $S_1 > S_2$ changes for the shear moduli of the $N_{1,2}$ to be compared.

The values of $\varepsilon_3$ are small compared with $\varepsilon_1$ and $|\varepsilon_2|$, and the corresponding curve $\varepsilon_3(\theta)$ is not given in the graph. Since it is the angular localizations of the extrema of $S$ and $\varepsilon_{1,2}$ (and the corresponding orientations of the eigenvectors) that are mainly important, the absolute values of $\varepsilon_{1,2}$ are not given; instead, a scale is used that is convenient for the perception. For the loop selected for an analysis, the condition $\xi_3 \parallel \Lambda_1$ is fulfilled at $\theta = \pm 180°$, i.e., for the points that lie in the plane of the loop. The same points are selected based on the condition of the maximum of the shear $S$. The maximum of the shear at $\theta = 0$ is associated with a small deviation of $\xi_3$ from $\Lambda_1$.

The purposes of this work do not require analyzing all specific features of the given dependences. We indicate only that the maximum of the shear modulus $S$ at $\theta_1 \approx \pm 180°$ (and also the region that includes the extrema of $\varepsilon_{1,2}$) corresponds to the orientation of the normal $N_1$ to the habit plane $\parallel \xi_{2\alpha} + \xi_{1\alpha}$ close to $[111]_\alpha$, upon the orientations of the eigenvectors $\xi_{1\alpha}$ and $\xi_{2\alpha}$ close to the orientations (14), namely,

$$L_1 = 7000,\ L_2 = 5000,\ \boldsymbol{b}_1 \parallel [1\bar{1}0]_\alpha,$$
$$\theta_1 = \pm 180°,\ Z = 0, \tag{48}$$
$$N_1(\theta_1) \parallel [0.576233\ 0.576157\ \overline{0.579654}]_\alpha,$$

$$\xi_{1\alpha}(\theta_1) = [\overline{0.0925686}\ 0.907431\ \overline{0.409877}]_\alpha,$$
$$\xi_{2\alpha}(\theta_1) = [0.907431\ \overline{0.0925686}\ \overline{0.409877}]_\alpha. \tag{49}$$

A comparison of (48), (49) with (35), (36) and (14) shows a satisfactory correspondence for the model set of elastic moduli (44).

In the case of $\boldsymbol{b}_2 \parallel [11\bar{1}]_\alpha$ and orientation $\Lambda_2 \parallel \boldsymbol{b}_2$, there is no θ for which the orientation of the $\xi_{3\alpha}$ axis be collinear to $[112]_\alpha$. Consequently, strictly speaking, such a DNC cannot initiate only the plane deformation of the plane $(112)_\alpha$. Nevertheless, for the case of minimum deviations of the vector $\xi_{3\alpha}$ from $[112]_\alpha$ (at $\theta \approx \pm 20°$, the deviation is $\approx \pm 3.4°$), the eigenvectors $\xi_{1\alpha}(\theta)$ and $\xi_{2\alpha}(\theta)$ are relatively close to the orientations obtained from (14) by the transposition of the first and third components, i.e., close to the vectors that determine the deformation axis of the mirror-symmetrical hexagonal cell. This result indicates that it is expedient to examine the intermediate (between $\boldsymbol{b}_1$ and $\boldsymbol{b}_2$) orientations of the Burgers vector $\boldsymbol{b}$, which can easily be enumerated systematically, taking linear combinations of $\boldsymbol{b}_1$ and $\boldsymbol{b}_2$. Then, for example, at $\boldsymbol{b}_3 \parallel [\bar{4}21]_\alpha$, $\Lambda_2 \parallel \boldsymbol{b}_3$, and $\theta \approx 19.59°$, the vector $\xi_{3\alpha} = [0.407221\ 0.407298$

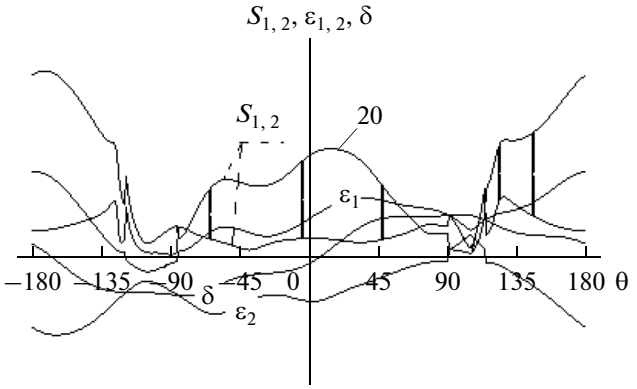


**Fig. 5.** Angular dependences of the magnitudes of the shears $S_{1,2}$, eigenvalues $\varepsilon_{1,2}$ of the tensor of deformations, and change in the relative volume δ of the elastic field of the DNC at $\boldsymbol{b}_3 \parallel [\bar{4}21]_\alpha$ for $R = 1200$.

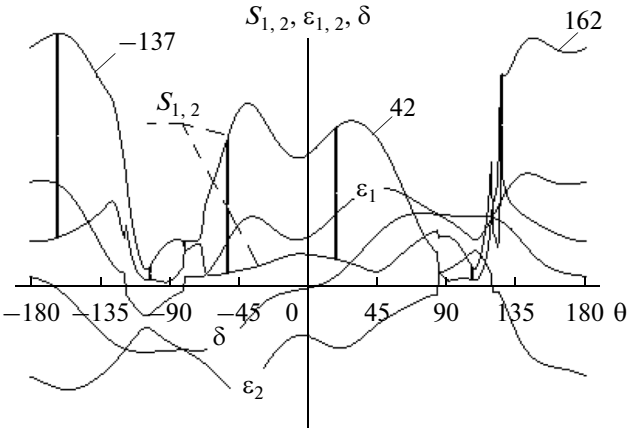


**Fig. 6.** Angular dependences of the magnitudes of the shears $S_{1,2}$, eigenvalues $\varepsilon_{1,2}$ of the tensor of deformations, and change in the relative volume δ of the elastic field of the DNC at $\boldsymbol{b}_4 \parallel [\bar{9}14]_\alpha$ for $R = 1200$.

$0.817484]_\alpha$ makes an angle ≈0.1° with $[112]_\alpha$, and the orientations (51) of the vectors $\xi_{1\alpha}$ and $\xi_{2\alpha}$ are noticeably nearer to the orientations (14) in comparison with (49) as follows:

$$L_1 = 7000, L_2 = 5000, \boldsymbol{b}_3 \parallel [\bar{4}21]_\alpha,$$
$$\theta = 19.59°, Z = 0, \quad (50)$$
$$N_1(\theta) \parallel [0.668048\ 0.477514\ \overline{0.570695}]_\alpha,$$
$$\xi_{1\alpha}(\theta) = [\overline{0.049953}\ 0.903651\ \overline{0.425346}]_\alpha,$$
$$\xi_{2\alpha}(\theta) = [0.911963\ \overline{0.132374}\ \overline{0.388331}]_\alpha. \quad (51)$$

It is important that the above angle θ belongs to the vicinity of the angles for which there are extrema of the shear and deformations, as can be seen from Fig. 5.

At $\boldsymbol{b}_4 \parallel [\bar{9}14]_\alpha$, $\Lambda_2 \parallel \boldsymbol{b}_4$, and θ ≈ 41.85°, the vector $\xi_{3\alpha} = [0.417948\ 0.417786\ 0.806706]_\alpha$ makes an angle of ≈1° with $[112]_\alpha$, and the orientations of the vectors $\xi_{1\alpha}$ and $\xi_{2\alpha}$ are nearer to the orientations (14) than (49), but farther from them than (51) as follows:

$$L_1 = 7000, L_2 = 5000, \boldsymbol{b}_4 \parallel [\bar{9}14]_\alpha,$$
$$\theta = 41.85°, Z = 0, k = 0.683, æ = 0.995, \quad (52)$$
$$N_1(\theta) \parallel [0.750340\ 0.341861\ \overline{0.565792}]_\alpha,$$
$$\xi_{1\alpha}(\theta) = [\overline{0.000085}\ 0.88800\ \overline{0.459843}]_\alpha,$$
$$\xi_{2\alpha}(\theta) = [0.908471\ \overline{0.192122}\ \overline{0.371173}]_\alpha. \quad (53)$$

Furthermore, the orientation of $\xi_{3\alpha}$ is close to $[112]_\alpha$ also at θ ≈ −137°, but in this case, the deviations of the vectors $\xi_{1\alpha}(\theta)$ and $\xi_{2\alpha}(\theta)$ from the axes (14) are noticeably greater than at θ = 41.85°.

Let us now discuss the possibility of the formation of IESs in the elastic field of a DNC that initiates the $\alpha \to \mathrm{IS}_{\alpha-\varepsilon}$ transition. First, note that the DNC that leads to the data given in (52) and (53) is completely acceptable for this aim. Indeed, at θ = 161.43°, the orientation of the axis $\xi_{3\alpha} = [0.410230\ 0.410206\ 0.81452]_\alpha$ makes an angle of 0.19° with $[112]_\alpha$. The data concerning the expected habit and the directions of the axes of deformations and macroshear are given in (54)–(56).

The vectors $\xi_{1\alpha}$ and $\xi_{2\alpha}$ (55) make an angle of ≈12.36° with the axes of symmetry. The angle θ = 161.43° belongs to the region of high values of shear $S_{2\alpha}$, which exceed the level of $S_{1\alpha}$ at θ = 41.85° (see Fig. 6). Therefore, the first to occur is most likely the transition to $\mathrm{IS}_{\alpha-\varepsilon}$ as follows:

$$L_1 = 7000, L_2 = 5000, \boldsymbol{b}_4 \parallel [\bar{9}14]_\alpha,$$
$$\theta = 161.43°, Z = 0, k = 1.088, æ = 0.968;$$
$$N_2(\theta) \parallel [\overline{0.321321}\ 0.900871\ \overline{0.291862}]_\alpha, \quad (54)$$
$$\xi_{1\alpha}(\theta) = [0.411257\ 0.713955\ \overline{0.566688}]_\alpha,$$
$$\xi_{2\alpha}(\theta) = [0.813989\ \overline{0.567450}\ \overline{0.124185}]_\alpha, \quad (55)$$
$$S_{2\alpha}(\theta) = [0.874727\ 0.0620628\ \overline{0.480626}]_\alpha. \quad (56)$$

Note that, at $\boldsymbol{b}_4 \parallel [\bar{9}14]_\alpha$ and θ = 161.43°, the misorientation between $\xi_{3\alpha}$ and $[112]_\alpha$ is by no means large. The orientation of $\boldsymbol{b}_4$ is close to that of the bisectrix between $\boldsymbol{b}_1$ and $\boldsymbol{b}_2$. The deviation from $\boldsymbol{b}_4$ increases the misorientation between $\xi_{3\alpha}$ and $[112]_\alpha$ for the angular localization of the vectors $\xi_{i\alpha}$ capable to initiate the $\alpha \to \mathrm{IS}_{\alpha-\varepsilon}$ transition. Thus, for example, at $\boldsymbol{b}_3 \parallel [\bar{4}21]_\alpha$, the deviation of the orientation of $\xi_{3\alpha}$ that is nearest to $[112]_\alpha$ at θ ≈ 141°, which is favorable for the $\alpha \to \mathrm{IS}_{\alpha-\varepsilon}$ transition, increases to ≈ 4.5°.

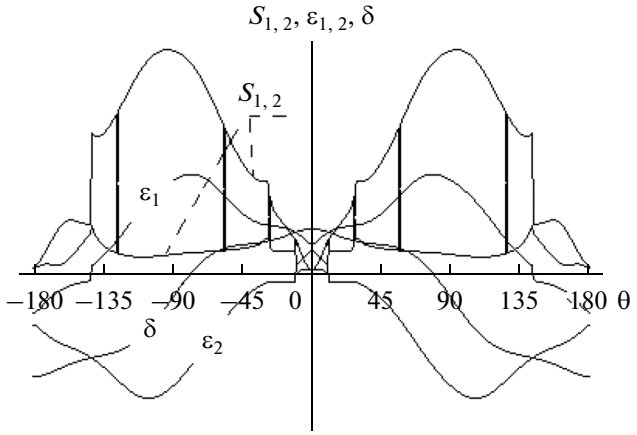


**Fig. 7.** Angular dependences of the magnitudes of the shears $S_{1,2}$, eigenvalues $\varepsilon_{1,2}$ of the tensor of deformations, and change in the relative volume δ of the elastic field of the DNC at $\boldsymbol{b}_1 \parallel [1\bar{1}0]_\alpha$ for $R = 1200$ in the case of a prismatic dislocation loop.

Note that, in equal measure, this DNC will favor the initiation of the $\alpha \rightarrow IS_{\alpha-\gamma}$ transition. After the analysis of DNCs in the form of rectangular glissile loops, let us examine a prismatic loop with segments $\Lambda_1 \parallel [112]_\alpha$ and $\Lambda_2 \parallel [11\bar{1}]_\alpha$ of the same dimensions as before, i.e., $L_1$ and $L_2$, for the Burgers vector $\boldsymbol{b} = \boldsymbol{b}_1 \parallel [1\bar{1}0]_\alpha$. The angular dependences of the characteristics of the elastic field of the DNC are given in Fig. 7.

The large values of the shear, as can be seen from Fig. 7, correspond to the vicinity of the angles $\theta = \pm 90°$. The maximum proximity of the vector $\xi_{3\alpha}$ to $[112]_\alpha$ is reached at $\theta \approx 90.84°$: $\xi_{3\alpha} = [0.417948\ 0.417786\ 0.806706]_\alpha$ makes an angle of $\approx 2.1°$ with $[112]_\alpha$. The orientations of the vectors $\xi_{1\alpha}$ and $\xi_{2\alpha}$ (58) are close to the orientations (14) as follows:

$$L_1 = 7000,\ L_2 = 5000,\ \boldsymbol{b}_1 \parallel [1\bar{1}0]_\alpha,$$
$$\theta = 90.84°,\ Z = 0,\ k = 0.897,\ æ = 0.997, \quad (57)$$
$$N_1(\theta) \parallel [0.663534\ 0.514289\ \overline{0.543350}]_\alpha,$$

$$\xi_{1\alpha}(\theta) = [\overline{0.034051}\ 0.913373\ \overline{0.405697}]_\alpha,$$
$$\xi_{2\alpha}(\theta) = [0.921733\ \overline{0.128214}\ \overline{0.366019}]_\alpha, \quad (58)$$

$$S_{1\alpha}(\theta) = [\overline{0.713069}\ 0.701057\ \overline{0.007232}]_\alpha. \quad (59)$$

Thus, in the case of the edge orientation of the Burgers vectors with respect to $\Lambda_1 \parallel [112]_\alpha$, the DNCs both in the form of glissile and sessile (prismatic) loops are capable of initiating the formation of IESs with acceptable characteristics for comparison with the initial idealized scheme of deformation of the plane $(112)_\alpha$.

## DISCUSSION OF THE RESULTS

The standard description of the deformation of the $(112)_\alpha$ plane for its transformation into plane $(0001)_\varepsilon$ with the use of homogeneous deformations requires the examination of two stages. In this case, the resulting deformations are large compared with the case of the deformation of the $(110)_\alpha$ plane. If the directions of the Burgers vectors are close to that of the bisectrix between the symmetry axes, for the DNCs in the form of glissile dislocation loops we can expect the sequence of the reconstruction of the type $\alpha \rightarrow IS \rightarrow \varepsilon$. In this case, according to (54), the orientations of the habits can be close to $\{131\}_\alpha$, which differs significantly from the estimations (38) and (39) for the habits close to $\sim\{021\}_\alpha$ obtained in the approximation of an elastically isotropic medium. Note that the difference indicated is caused mainly by deviations of the axes of deformation from the axes of symmetry rather than by the allowance for anisotropy.

Since the $\{112\}_\alpha$ planes are not symmetry planes, as a rule, their plane deformation of the tension–compression type cannot be initiated by the elastic field of a DNC in the anisotropic medium. Therefore, there are grounds to assume that the degree of deviation from the parallelism of planes in MORs (32) must exceed similar misorientations in the MORs (6), (7). Moreover, since $\{110\}_\alpha$ are the symmetry planes, a strict parallelism of planes in the MORs (6), (7) can be expected.

If the orientations of the Burgers vectors of the DNC are close to $\langle 1\bar{1}0\rangle_\alpha$, then the $\alpha \rightarrow \varepsilon' \rightarrow \varepsilon$ transition is preferable, where the designation ε' refers to the distorted ε phase. In this case, according to (48), (49), the habits $\{hkl\}_\alpha$ close to $\{111\}_\alpha$ are expected, which agrees satisfactorily with the orientations (35) found based on the approximation of the elastically isotropic medium.

The problem of the magnitude of the lattice parameter $a_\varepsilon$ upon the $\{112\}_\alpha \rightarrow \{0001\}_\varepsilon$ transformation is of great interest. As was shown above, here the common value $a_\varepsilon < a_\alpha$ can be realized due to the compressive deformation caused by the expansion of the unstable state $IS1_{\alpha-\gamma}$. However, under the conditions of the formation of the ε phase independent of the γ phase, in accordance with the requirement of the minimum time necessary for the formation of crystals of the ε phase, we can expect the formation of the variant where $a_\varepsilon > a_\alpha$. Indeed, for the ideal lattice of the ε phase that arise from the $IS1_{\alpha-\varepsilon}$, the parameter $a_\varepsilon$ is written as follows:

$$a_\varepsilon = a_\alpha(1 - |\varepsilon_2|_2)\sqrt{11}/2. \quad (60)$$

In the approximation of an isotropic medium, according to (18), $|\varepsilon_2|_2 = |\varepsilon_{2f}| \approx 0.32$; then, from (60) we find

$$a_\varepsilon = a_{\varepsilon 2} \approx 1.128\ a_\alpha > a_\alpha. \quad (61)$$

Recall [5, 6] that, upon the transformation $\{110\}_\alpha \to \{0001\}_\varepsilon$, we have

$$a_\varepsilon = a_{\varepsilon 1} = a_\alpha (1 - |\varepsilon_2|_1) < a_\alpha. \quad (62)$$

It follows from (61) and (62), that there is an opportunity for fragments of the ε phase with different values of the lattice parameter to exist in different regions of the material. If this opportunity is realized, two different parameters of the γ phase can also appear, since the ε–γ MT, just as the γ–ε MT [12] can be realized via the shuffling of the close-packed planes without a change in the macroscopic morphological characteristics, leading to the following relation:

$$a_\gamma = \sqrt{2} a_\varepsilon. \quad (63)$$

It is worth of noting that a similar conclusion also follows for the anisotropic medium in the approximation of longitudinal waves with the wave normals along the directions (14), since the wave velocities in these directions, which substantially deviate from the symmetry axes, are close to each other; this means that we should expect the proximity of the magnitudes of deformations of tension and compression as well.

If the opportunity of the formation of the ε phase with the lattice parameter $a_{\varepsilon 2} > a_{\varepsilon 1}$ is not realized, this means that, in the nanocrystalline state under the conditions of slow heating at comparatively high temperatures, a minimum, almost equilibrium value of the parameter $a_\varepsilon \approx a_{\varepsilon 1} \approx a_{\varepsilon 2}$ is established.

## CONCLUSIONS

A condition has been found concerning the connection between the tension and compression deformations in orthogonal directions $\xi_{1,2}$ that lie in the $\{112\}_\alpha$ planes upon the transformation of planes $\{112\}_\alpha$ into the basal planes $\{0001\}_\varepsilon$.

Since the $\{112\}_\alpha$ planes, in contrast to $\{110\}_\alpha$, are not the symmetry planes, in the MORs-3 (32), a misorientation is expected between the $\{112\}_\alpha$ and $\{0001\}_\varepsilon$ planes, which depends on the type of DNCs that initiate the process of the appearance of IESs.

From the viewpoint of the experimental verification, a conclusion on the opportunity of the existence of two values of the lattice parameter $a_\varepsilon$ of the ε phase in the same alloy is of great interest.

The estimates performed make it possible to propose an explanation for one of important features [10] of the reverse α–ε–γ MTs, which consists in the proximity of the orientations of the planes of three phases: $\{112\}_\alpha \| \{0001\}_\varepsilon \| \{112\}_\gamma$. The explanation reduces to the assumption on the formation of a specific intermediate state, whose instability leads to the concerted formation of the γ and ε phases in the conjugated regions.

Thus, the allowance for the opportunity of the occurrence of the α–ε MT via the transformation of $\{112\}_\alpha$ planes into the basal planes $\{0001\}_\varepsilon$ substantially supplements the results of the dynamic theory [8] that relate to the mechanism of the α–ε–γ MTs in the Fe–32Ni alloy.

Concerning the prospects for the nearest studies, note that the scenarios with an increase in the values of the lattice parameter upon the α–ε–γ MTs can be implemented under the conditions of an excess free volume, which appears upon the irradiation of the α phase of iron alloys both with the transformation of $(110)_\alpha$ and $(112)_\alpha$ planes.

## ACKNOWLEDGMENTS

Some of the results of this work has been presented in a brief form in [19]. The authors are grateful to the participants of the 13 International Conference on the Dislocation Structure and Mechanical Properties of Metals and Alloys DSMPMA-2014 for a fruitful discussion of the results of this work and for useful remarks. This work was supported in part by the Russian Foundation for Basic Research, project no. 14-08-00734).

## REFERENCES

1. M. P. Kashchenko and V. G. Chashchina, "Dynamic model of supersonic martensitic crystal growth," Phys.-Usp. **54**, 331–349 (2011).
2. M. P. Kashchenko and V. G. Chashchina, "Martensitic crystal formation in the limiting case of supersound speed growth," Pis'ma Mater. **1**, 7–15 (2011).
3. M. P. Kashchenko and V. G. Chashchina, "Fundamental achievements of the dynamic theory of reconstructive martensitic transformations," Mater. Sci. Forum **738–739**, 3–9 (2013).
4. M. P. Kashchenko, *Wave Model of Martensitic Growth at γ–α Transformation in Iron-Based Alloys*, 2nd ed. (NITs "Regul. i Khat. Dinam." Izhevsk. Inst. Komp'yut. Tekhnol., Izhevsk, 2010) [in Russian].
5. M. P. Kashchenko and V. G. Chashchina, "Crystal dynamics of the bcc–hcp martensitic transformation: I. Controlling wave process," Phys. Met. Metalogr. **105**, 537–543 (2008).
6. M. P. Kashchenko and V. G. Chashchina, "Crystal dynamics of the bcc–hcp martensitic transformation: II. Morphology," Phys. Met. Metallogr. **106**, 14–23 (2008).
7. M. P. Kashchenko and V. G. Chashchina, *Dynamic Model of Twinned Martensitic Crystals at γ–α Transformation in Iron Alloys* (UGLTU, Ekaterinburg, 2009) [in Russian].
8. M. P. Kashchenko and V. G. Chashchina, "Dynamic theory of morphological characteristics of ε and γ phase crystals, including Headley–Brooks orientation relationships at α–ε and α–ε–γ martensitic transformations," Phys. Met. Metallogr. (2015), see this issue.
9. I. G. Kabanova, V. V. Sagaradze, N. V. Kataeva, and V. E. Danil'chenko, "Detection of the ε phase and the Headley–Brooks orientation relationships upon α–γ transformation in the Fe–32% Ni alloy," Phys. Met. Metallogr. **112**, 381–388 (2011).
10. V. V. Sagaradze, N. V. Kataeva, I. G. Kabanova, V. A. Zavalishin, A. I. Valiullin, and M. F. Klyukina,

"Structural mechanism of reverse $\alpha \rightarrow \gamma$ transformation and strengthening of Fe–Ni alloys," Phys. Met. Metallogr. **115**, 661–671 (2014).

11. T. J. Headley and J. A. Brooks, "A New bcc–fcc orientation relationship observed between ferrite and austenite in solidification structures of steels," Metal. Mater. Trans. A **33**, 5–15 (2002).
12. V. G. Chashchina, "A modified dynamic model of an fcc–hcp martensitic transformation without macroshear," Russ. Phys. J. **52**, 763–765 (2009).
13. W. Harrison, *Electronic Structure and the Properties of Solids* (Freeman, San Francisco, 1980; Mir, Moscow, 1983).
14. D. A. Mirzaev, O. P. Morozov, and M. M. Shteinberg, "On the connection of transformations in iron and its alloys," Fiz. Met. Metalloved. **36**, 560–568 (1973).
15. M. P. Kashchenko, A. G. Semenovykh, and V. G. Chashchina, "The lower temperature boundary of the onset of the formation of $\alpha$-martensite upon cooling in iron-based alloys," Phys. Met. Metallogr. **95**, 116–121 (2003).
16. M. P. Kashchenko, V. G. Chashchina, and S. V. Vikharev, "Dynamic model of the formation of twinned martensite crystals: I. Control wave process and the removal of degeneracy in twin-boundary orientation," Phys. Met. Metallogr. **110**, 200–209 (2010).
17. M. P. Kashchenko, V. G. Chashchina, and S. V. Vikharev, "Dynamic model of the formation of twinned martensite crystals: II. Pretransition states and relationships between the volumes of the twin components," Phys. Met. Metallogr. **110**, 305–317 (2010).
18. M. P. Kashchenko and V. G. Chashchina, "Key role of transformation twins in comparison of results of crystal geometric and dynamic analysis for thin-plate martensite," Phys. Met. Metallogr. **114**, 821–825 (2013).
19. M. P. Kashchenko and V. G. Chashchina, in *Proc. 13th Int. Conf. "DSMSMS-2014* (Ural Branch, Russian Academy of Sciences, Ekaterinburg, 2014), pp. 166–168.

*Translated by S. Gorin*